

# Growth and characterization of $\text{YBa}_2\text{Cu}_3\text{O}_x$ and $\text{NdBa}_2\text{Cu}_3\text{O}_x$ superconducting thin films by mist microwave-plasma chemical vapor deposition using a $\text{CeO}_2$ buffer layer

N. TAKAHASHI

*Department of Materials Science, Shizuoka University, Hamamatsu, Shizuoka 432-8561, Japan*

A. KOUKITU, H. SEKI

*Department of Applied Chemistry, Tokyo University of Agriculture and Technology, Koganei, Tokyo 184, Japan*

Superconducting thin films of  $\text{YBa}_2\text{Cu}_3\text{O}_x$  (YBaCuO) and  $\text{NdBa}_2\text{Cu}_3\text{O}_x$  (NdBaCuO) were grown by mist microwave-plasma chemical vapor deposition (MPCVD) using a  $\text{CeO}_2$  buffer layer on a MgO (001) substrate. In this method, the  $\text{CeO}_2$  buffer layer was deposited on the MgO (001) substrate at 1173 K by MPCVD. YBaCuO and NdBaCuO films were then grown at 1073 K and 1223 K, respectively. The  $T_c$  (zero resistance) values of the YBaCuO and NdBaCuO films obtained with a  $\text{CeO}_2$  buffer layer were 90.1 K and 94.1 K, respectively, about 10 K higher than those without a  $\text{CeO}_2$  buffer layer. The surface roughness of the films was less than 5 nm in each case. The interface between the substrate and the grown layer was confirmed to be extremely sharp by Auger profile analysis. © 2000 Kluwer Academic Publishers

## 1. Introduction

High-temperature superconductor YBaCuO thin films have been successfully deposited on highly chemically reactive substrates (such as silicon or sapphire) using a variety of techniques and buffer layers since the discovery of these new high-temperature superconducting materials. In particular, the buffer layer is useful for the growth of high-quality superconducting thin films and epitaxial growth of various materials. In recent years,  $\text{CeO}_2$  has become a popular material for use as a buffer and barrier layer for high- $T_c$  superconductors, YBaCuO [1], BiSrCaCuO [2] and TlBaCaCuO [3] films.  $\text{CeO}_2$  has a fluorite structure with a lattice constant of 0.541 nm at room temperature. By rotating the  $\text{CeO}_2$  basal plane by  $45^\circ$ , the lattice mismatch is 0.16% and 1.7% along the  $a$  and  $b$  axis of YBaCuO, respectively [1]. Therefore,  $\text{CeO}_2$  thin films have been used as a buffer layer for YBaCuO films and as template layers for formation of a bi-epitaxial Josephson junction [4].

In a previous paper we reported the new technique, mist microwave-plasma chemical vapor deposition (MPCVD) [5]. This method possesses several technological advantages. In particular simple preparation of thin films of various materials utilizing an aqueous solution of nitrate materials as the source is possible. We have succeeded in preparing YBaCuO [6, 7], BiSrCaCuO [8, 9], TlBaCaCuO [10, 11] and NdBaCuO [12] superconducting thin films. However, the preparation of superconducting thin films by MPCVD using a

$\text{CeO}_2$  buffer layer has not yet been performed. In particular, the preparation of a NdBaCuO superconducting thin film using a buffer layer has not yet been reported in the superconductor field. In this paper, we report the growth and characterization of YBaCuO and NdBaCuO superconducting thin films by MPCVD using a  $\text{CeO}_2$  buffer layer on MgO substrate.

## 2. Experimental

The MPCVD system with a microwave generator and an ultrasonic wave oscillator were used in the growth of thin films. The  $\text{CeO}_2$  buffer layer and YBaCuO film were grown by normal MPCVD [6], and the NdBaCuO film was grown by dual-sources MPCVD. The schematic diagram of the MPCVD system with dual-sources is shown in Fig. 1. The sources for the superconductor were prepared by dissolving metal nitrates in deionized water. In the case of NdBaCuO growth, the solution of  $\text{Nd}(\text{NO}_3)_3$  and  $\text{Ba}(\text{NO}_3)_2\text{-Cu}(\text{NO}_3)_2$  in the dual-sources MPCVD were supplied from separate bottles. The substrate used was a MgO (001) single crystal. Prior to deposition, the MgO substrate was mirror-polished using 0.25  $\mu\text{m}$  diamond paste and was then heated to 1050  $^\circ\text{C}$  in a furnace for 2.5 hours in air. The mean square roughness ( $R_{\text{ms}}$ ) in a  $30 \times 30 \mu\text{m}$  square of the MgO substrate was less than 0.4 nm. Typical growth conditions for the  $\text{CeO}_2$  buffer layer and the superconducting thin film are

TABLE I Typical growth conditions

	CeO <sub>2</sub>	YBaCuO	NdBaCuO
Total metal concentration in solution	0.2 mol/l	0.4 mol/l	0.2 mol/l
Atomic ratio	—	1:2:3	1:2:3
Substrate	MgO (001)	MgO (001), CeO <sub>2</sub> /MgO (001)	MgO (001), CeO <sub>2</sub> /MgO (001)
Microwave power (substrate temperature)	350 W (1173 K)	300 K (1073 K)	350 W (1223 K)
Ultrasonic power of mist generator	14 W	14 W	14 W
Mist supply rate	80 sccm	80 sccm	80 sccm
Total carrier gas flow rate	300 sccm	300 sccm	300 sccm
Input molar ratio of oxygen	0.3	0.3	0.5
Total pressure of reactor	50 Torr	50 Torr	50 Torr
Duration of deposition	0.5 hours	5 hours	5 hours

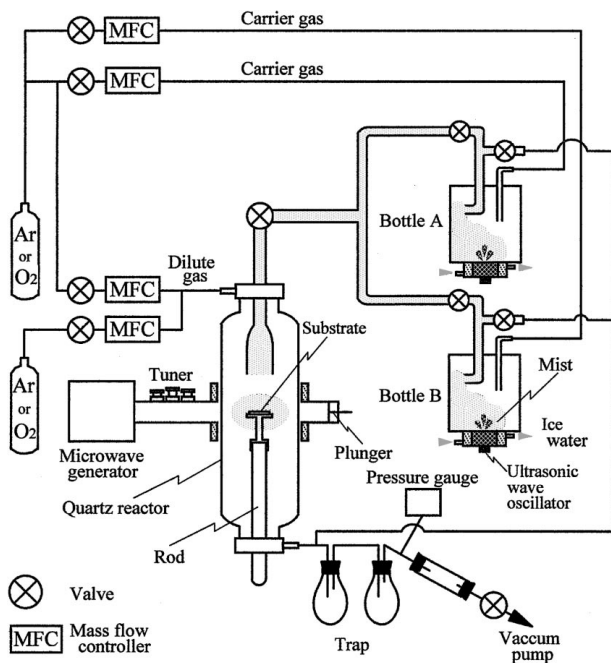


Figure 1 Schematic diagram of MPCVD with dual-source.

summarized in Table I. In order to investigate the effect of the CeO<sub>2</sub> buffer layer, the growth of superconducting thin film without a buffer layer was carried out under the same conditions. The temperature of the substrate was measured by means of an optical pyrom-

eter. In addition, the substrate temperature was calibrated by a thermocouple inserted into the back of the susceptor. A mist of the source solution (particle size, 1–2 μm), produced by an ultrasonic mist generator, was introduced into the reactor using Ar as the carrier gas. Microwave (2.45 GHz) power was supplied by a magnetron generator. The supply rate of the mist was determined by the flow rate of the carrier gas. The total flow rate of O<sub>2</sub> and Ar in the reactor was 300 standard cubic centimeters (sccm). The introduction of oxygen into reactor was necessary for the oxidative reaction. The input molar ratio of oxygen, O<sub>R</sub> is defined hereafter as

$$O_R = \frac{F_{\text{oxygen species}}}{(F_{\text{oxygen species}} + F_{\text{Ar}})} \quad [8],$$

where  $F_{\text{oxygen species}}$  is the flow rate of O<sub>2</sub> gas, and  $F_{\text{Ar}}$  is the flow rate of Ar gas.

Fig. 2a and b show the YBaCuO and NdBaCuO film growth processes using a CeO<sub>2</sub> buffer layer. The growth progresses through two stages. In the first stage, the CeO<sub>2</sub> buffer layer was grown for 30 minutes at 1173 K. The thickness of the CeO<sub>2</sub> buffer layer was 50 nm. The temperatures were then changed to the growth temperature of YBaCuO (1073 K) and NdBaCuO (1223 K) films, respectively. In the second stage, the growth of the superconducting thin films was initiated by supplying mist into the reactor, and the films were grown

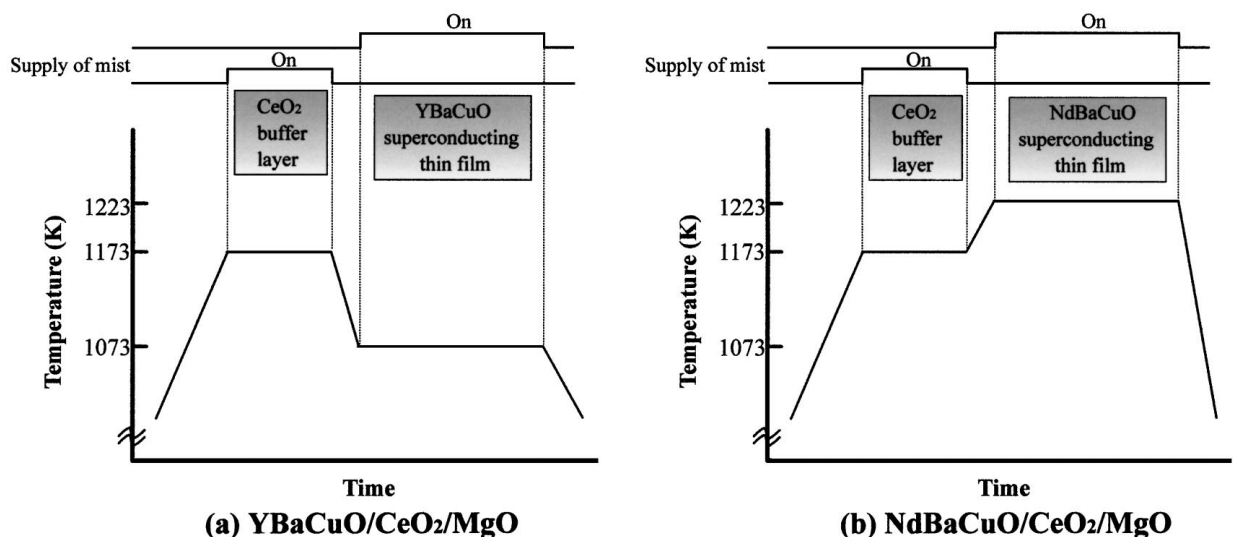


Figure 2 Time chart schematically illustrating the growth process of YBaCuO and NdBaCuO films by MPCVD using a CeO<sub>2</sub> buffer layer.

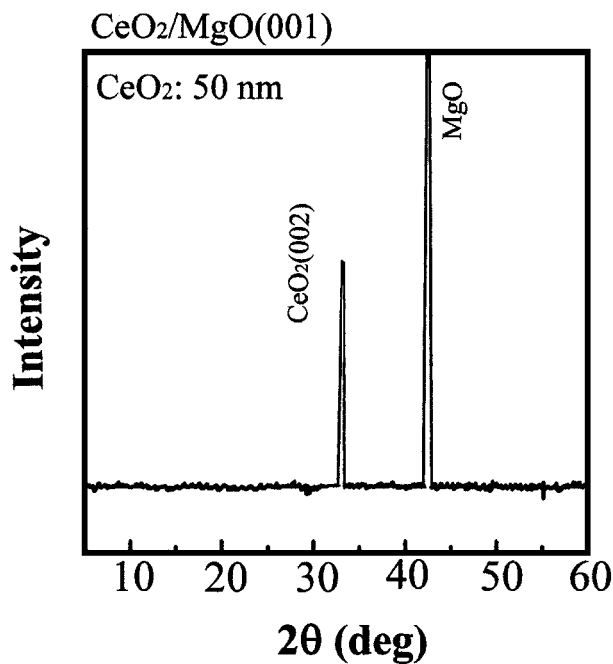


Figure 3 X-ray diffraction pattern for the CeO<sub>2</sub> buffer layer deposited on a MgO (001) substrate.

for 5 hours at the each temperature. The thickness of YBaCuO and NdBaCuO films obtained was about 650 nm.

An X-ray diffractometer with CuK<sub>α</sub> radiation in the 2θ range from 0 to 60° was used for characterization of the as-grown films. X-ray diffraction patterns of the film were measured using a diffractometer operating at 25 kV with a filament current of 20 mA, using a nickel filter for CuK<sub>α</sub> radiation. The chemical compositions of the as-grown films were investigated by electron-probe X-ray microanalysis (EPMA), using a probe 1 μm in diameter, a probe current of 3 × 10<sup>-8</sup> A, and an accelerating voltage of 15 kV. The surface morphology and thickness of the resultant films were observed by atomic force microscopy (AFM) and scanning electron microscopy (SEM), respectively. The film composition was profiled in depth by Auger electron spectroscopy (AES). Electrical resistivity was measured using the standard four-probe method with silver paint contacts

for as-grown films over a range of temperatures from 50 to 300 K.

### 3. Result and discussion

#### 3.1. Growth of CeO<sub>2</sub> buffer layers

Prior to investigating the effect of a CeO<sub>2</sub> buffer layer for the growth of superconducting thin films, the CeO<sub>2</sub> buffer layer was characterized by X-ray diffraction (XRD) and atomic force microscopy (AFM). Fig. 3 shows an X-ray diffraction profile of the CeO<sub>2</sub> buffer layer. A strong diffraction peak at 33.1° corresponding to (002) of CeO<sub>2</sub> buffer layer can be seen for the as-grown layer. The peak at 42.9° is assigned to the (002) diffraction of the MgO substrate. From this result, it can be seen that the CeO<sub>2</sub> buffer layer can be grown successfully by MPCVD. The full width at half maximum (FWHM) value of the (002) CeO<sub>2</sub> peak of the as-grown layer was about 9.0 minutes.

The surface morphology of the CeO<sub>2</sub> buffer layer was observed from the AFM image. The AFM image is shown in Fig. 4 with the corresponding surface roughness. *R*<sub>ms</sub> in a 30 × 30 μm square of the CeO<sub>2</sub> buffer layer was less than 0.4 nm. From this result, it is clear that the surface of the CeO<sub>2</sub> buffer layer is very smooth.

#### 3.2. Growth of YBaCuO superconducting thin films

The effect of a CeO<sub>2</sub> buffer layer on the growth of YBaCuO superconducting thin films was investigated. The X-ray diffraction patterns from the YBaCuO superconducting thin film with and without the CeO<sub>2</sub> buffer layer are shown in Fig. 5a and b, respectively. The diffraction intensities of the (00*l*) reflections for the YBaCuO films with CeO<sub>2</sub> buffer layer are stronger than those without the CeO<sub>2</sub> buffer layer. The FWHM values of the (006) peak for the YBaCuO film without the CeO<sub>2</sub> buffer layer was about 31.5 minutes, while that of the film with the CeO<sub>2</sub> buffer layer was about 13.4 minutes. This result shows that the CeO<sub>2</sub> buffer layer promotes the crystallization of YBaCuO superconducting thin films together with *c*-axis orientation. The composition of the YBaCuO films obtained on a CeO<sub>2</sub> buffer layer was determined to be Y<sub>0.99</sub>Ba<sub>1.98</sub>Cu<sub>2.98</sub>O<sub>*x*</sub> using EPMA analysis.

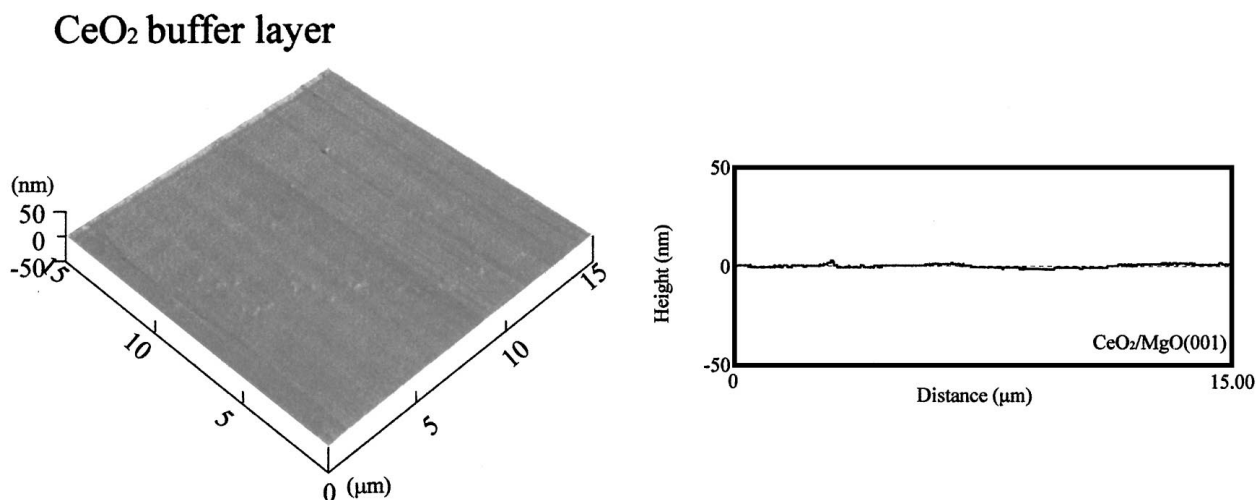


Figure 4 AFM image and line profile of the CeO<sub>2</sub> buffer layer on a MgO (001) substrate.

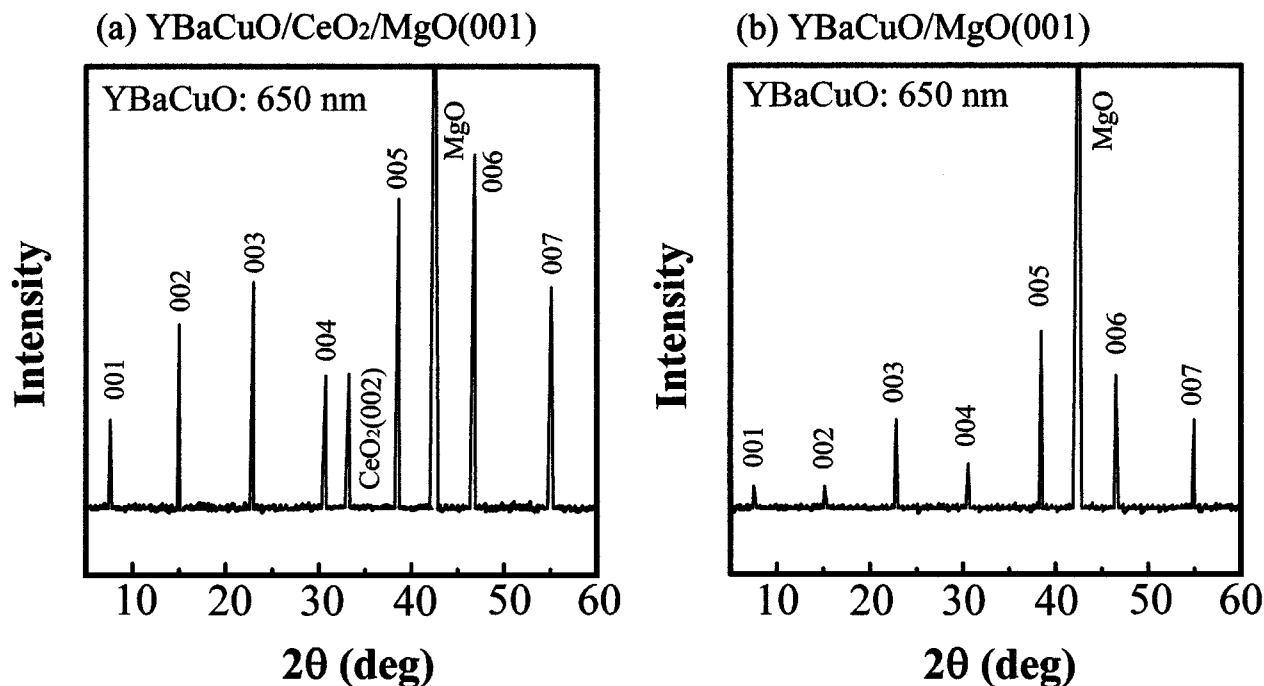


Figure 5 X-ray diffraction pattern for YBaCuO films (a) with a CeO<sub>2</sub> buffer layer, and (b) without a CeO<sub>2</sub> buffer layer.

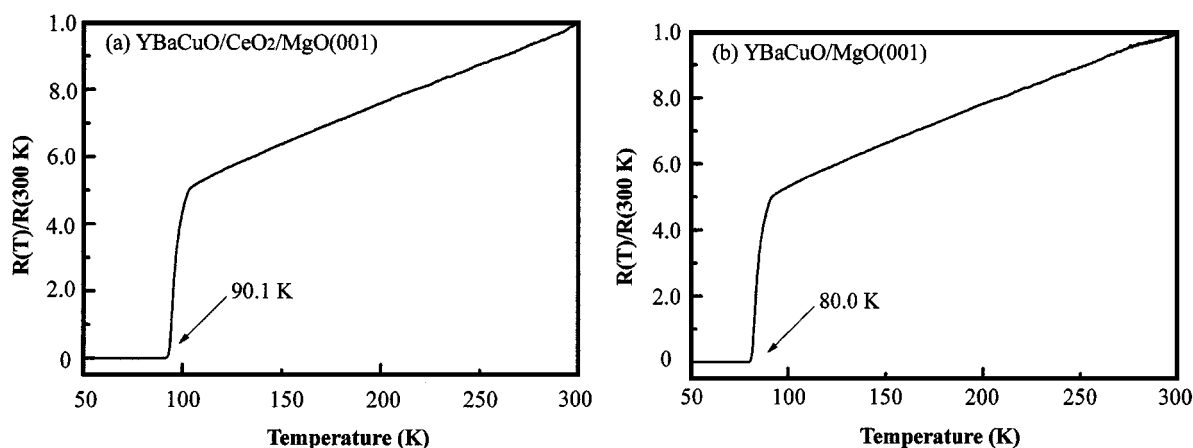


Figure 6 Resistance normalized at 300 K versus temperature for YBaCuO film (a) with a CeO<sub>2</sub> buffer layer, and (b) without a CeO<sub>2</sub> buffer layer.

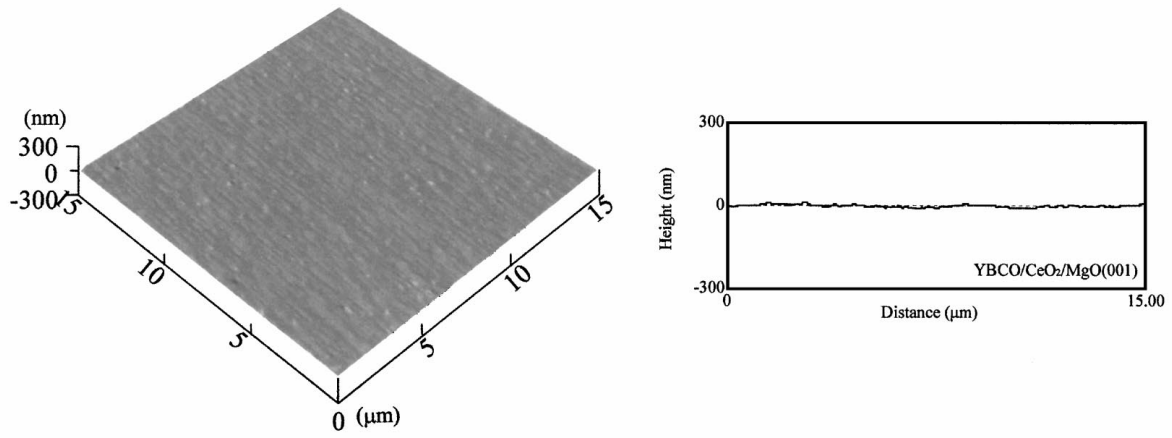
Fig. 6a and b show the electrical resistance normalized at 300 K versus temperature of the YBaCuO thin film obtained with and without a CeO<sub>2</sub> buffer layer, respectively. The resistivities at 300 K of the YBaCuO superconducting thin films with and without the CeO<sub>2</sub> buffer layer were 3.4 mΩ cm and 24.5 mΩ cm, respectively. The  $T_c$  value of YBaCuO film obtained with the CeO<sub>2</sub> buffer layer was 90.1 K. This  $T_c$  value is about 10 K higher than that of the same material without a CeO<sub>2</sub> buffer layer. As previously described in Fig. 5, the CeO<sub>2</sub> buffer layer promotes crystallization of YBaCuO superconducting thin films together with *c*-axis orientation. Consequently, the increase of  $T_c$  value may be attributable to the enhancement of the crystalline quality of the YBaCuO superconducting thin film in the case when a CeO<sub>2</sub> buffer layer was used. However, the exact reason is not well understood at present.

The AFM images of the YBaCuO superconducting thin film with and without the CeO<sub>2</sub> buffer layer

are shown in Fig. 7a and b, respectively with the corresponding surface roughness. The surface of the YBaCuO film with CeO<sub>2</sub> buffer layer was much smoother than that of the film without.  $R_{ms}$  in a 30 × 30 μm square of the obtained YBaCuO film on a CeO<sub>2</sub> buffer layer was less than 5 nm. Consequently, the use of a CeO<sub>2</sub> buffer layer is useful for growing high-quality YBaCuO superconducting thin films.

Fig. 8 shows the AES depth profile of the YBaCuO superconducting thin film prepared with and without CeO<sub>2</sub> buffer layer. As can be seen from Fig. 8b, it was found that Mg diffused into the YBaCuO layer in the thin film obtained without a CeO<sub>2</sub> buffer layer. On the other hand, the interfaces between YBaCuO and CeO<sub>2</sub>, and CeO<sub>2</sub> and MgO are also very sharp, as shown in Fig. 8a. The results of the Auger depth profile of YBaCuO with CeO<sub>2</sub> buffer layer suggest that the CeO<sub>2</sub> buffer layer may be a good candidate for the tunnel barrier needs in superconductor/insulator/superconductor devices.

(a) YBaCuO/CeO<sub>2</sub>/MgO(001)



(b) YBaCuO/MgO(001)

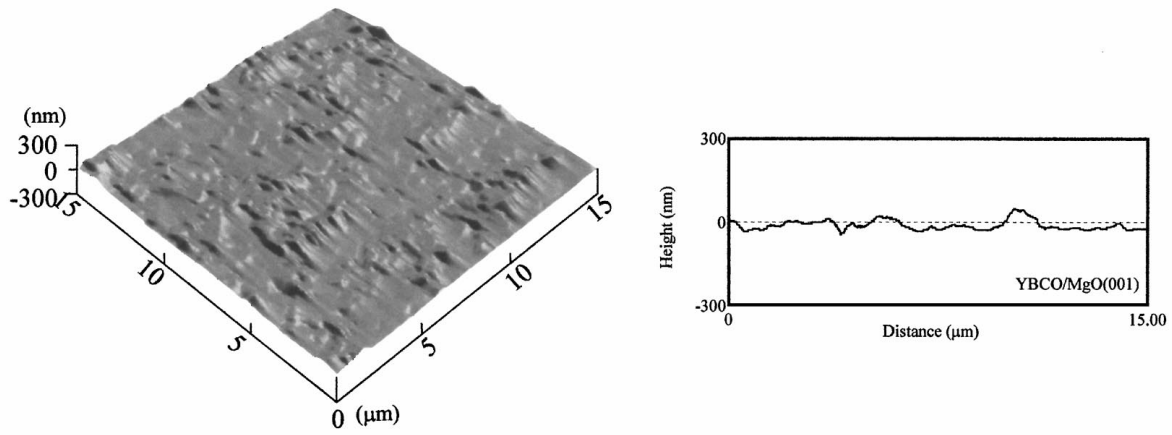
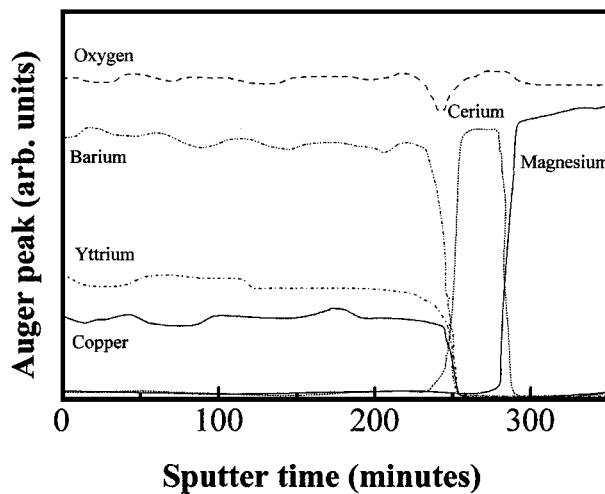


Figure 7 AFM image and line profile of a YBaCuO film (a) with a CeO<sub>2</sub> buffer layer, and (b) without a CeO<sub>2</sub> buffer layer.

(a) YBaCuO/CeO<sub>2</sub>/MgO(001)



(b) YBaCuO/MgO(001)

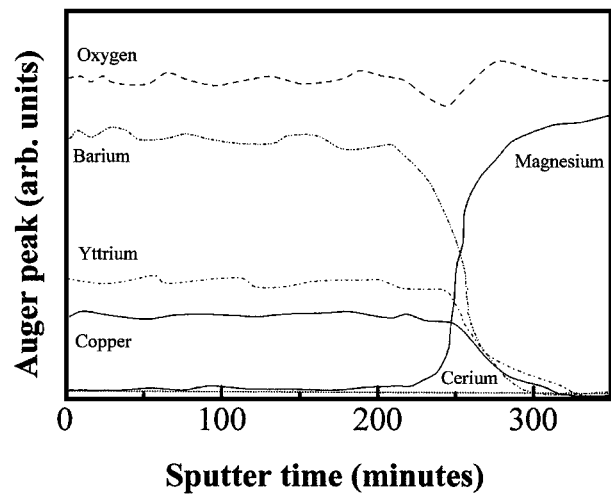


Figure 8 Auger electron spectroscopy depth profile of a YBaCuO film on MgO substrate (a) with a CeO<sub>2</sub> buffer layer and (b) without a CeO<sub>2</sub> buffer layer.

### 3.3. Growth of NdBaCuO superconducting thin films

The effect of a CeO<sub>2</sub> buffer layer on the growth of NdBaCuO superconducting thin films was investigated. The X-ray diffraction patterns from the NdBaCuO

superconducting thin film with and without the CeO<sub>2</sub> buffer layer are shown in Fig. 9a and b, respectively. As shown in Fig. 9, the enhanced intensities of the (00 $l$ ) reflections for all the films indicate that the  $c$ -axis are preferentially oriented perpendicular to the MgO

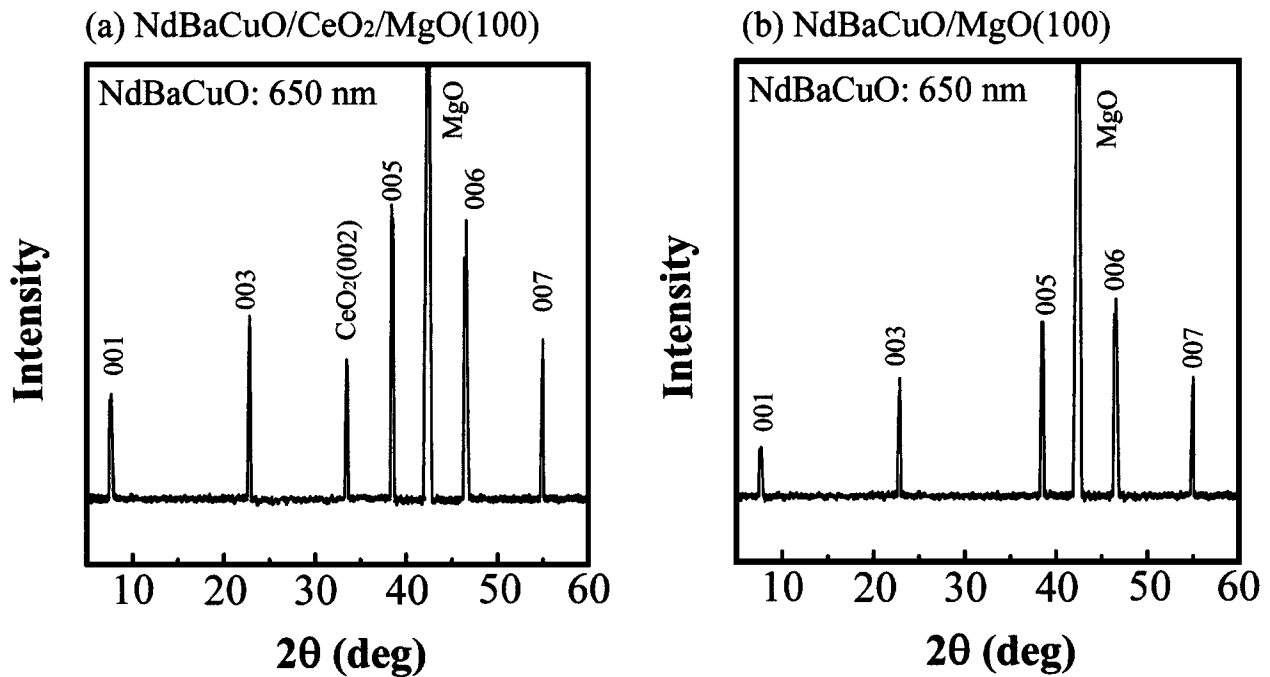


Figure 9 X-ray diffraction pattern for YBaCuO films (a) with a CeO<sub>2</sub> buffer layer, and (b) without a CeO<sub>2</sub> buffer layer.

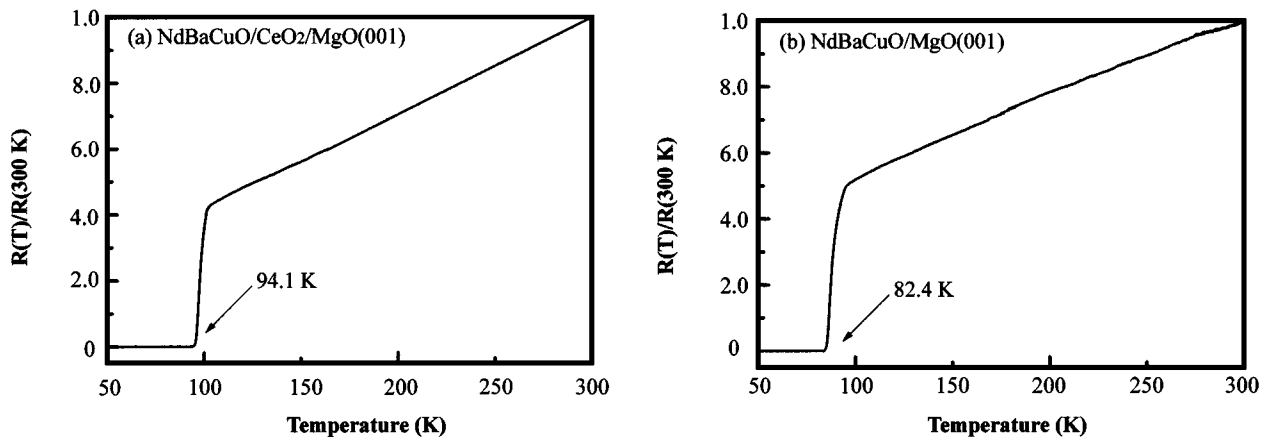


Figure 10 Resistance normalized at 300 K versus temperature for a NdBaCuO film (a) with a CeO<sub>2</sub> buffer layer, and (b) without a CeO<sub>2</sub> buffer layer.

(001) substrate surface. In particular, it is found that the diffraction intensities of the (00*l*) reflections for the NdBaCuO films with the CeO<sub>2</sub> buffer layer are stronger than those without the CeO<sub>2</sub> buffer layer. This result is similar to that obtained for the YBaCuO superconducting thin film. The FWHM values of the (006) peak for the NdBaCuO film without the CeO<sub>2</sub> buffer layer was about 40.3 minutes, however, that of the film with the CeO<sub>2</sub> buffer layer was about 15.6 minutes. This result shows that the CeO<sub>2</sub> buffer layer promotes crystallization of NdBaCuO superconducting thin films together with *c*-axis orientation. The composition of the NdBaCuO films obtained on a CeO<sub>2</sub> buffer layer was determined to be Nd<sub>1.01</sub>Ba<sub>2.01</sub>Cu<sub>3.00</sub>O<sub>x</sub> using EPMA analysis.

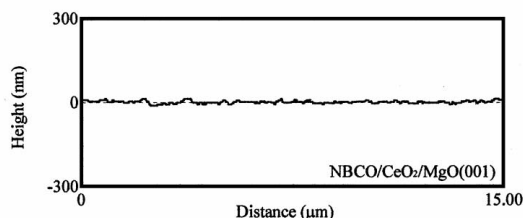
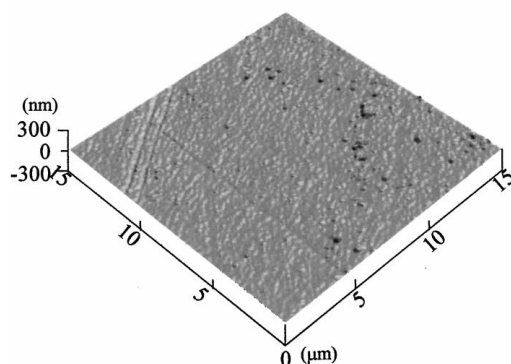
Fig. 10a and b show the electrical resistance normalized at 300 K versus temperature of the NdBaCuO thin film with and without a CeO<sub>2</sub> buffer layer, respectively. The resistivity at 300 K of the YBaCuO superconducting thin films with and without the CeO<sub>2</sub> buffer layer were 1.50 mΩ cm and 20.0 mΩ cm, respectively. This

*T<sub>c</sub>* value is about 10 K higher than that of the same material without a CeO<sub>2</sub> buffer layer. The increase of *T<sub>c</sub>* value may be attributable to the enhancement of the crystalline quality of the NdBaCuO superconducting thin film in the case when a CeO<sub>2</sub> buffer layer was used.

The AFM images of the NdBaCuO superconducting thin film with and without the CeO<sub>2</sub> buffer layer are shown in Fig. 11a and b, respectively with the corresponding surface roughness. The surface of the NdBaCuO film with CeO<sub>2</sub> buffer layer was much smoother than that of the film without. *R<sub>rms</sub>* in a 30 × 30 μm square of the obtained NdBaCuO film on a CeO<sub>2</sub> buffer layer was less than 5 nm. Consequently, the use of the CeO<sub>2</sub> buffer layer is useful for growing high-quality YBaCuO superconducting thin films.

Fig. 12 shows the AES depth profile of the NdBaCuO superconducting thin films prepared with and without a CeO<sub>2</sub> buffer layer and with CeO<sub>2</sub> buffer layer. In analogy with YBaCuO superconducting thin films, the interfaces between NdBaCuO and CeO<sub>2</sub>, and CeO<sub>2</sub> and MgO are extremely sharp. The interdiffusion

(a) NdBaCuO/CeO<sub>2</sub>/MgO(001)



(b) NdBaCuO/MgO(001)

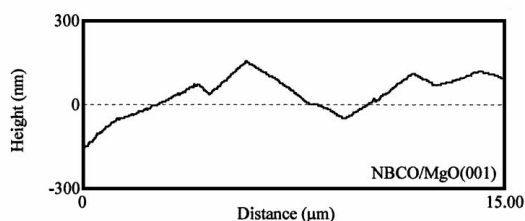
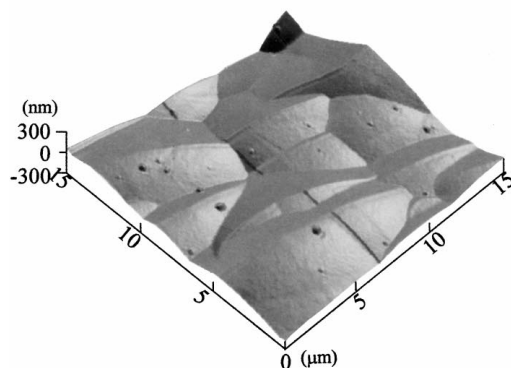
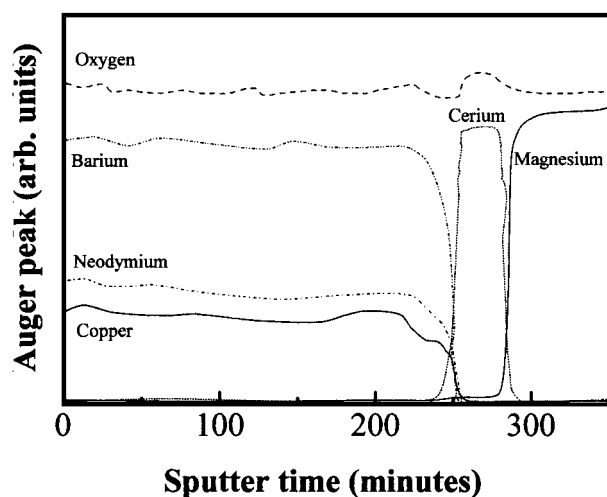


Figure 11 AFM image and line profile of a NdBaCuO film (a) with a CeO<sub>2</sub> buffer layer, and (b) without a CeO<sub>2</sub> buffer layer.

(a) NdBaCuO/CeO<sub>2</sub>/MgO(001)



(b) NdBaCuO/MgO(001)

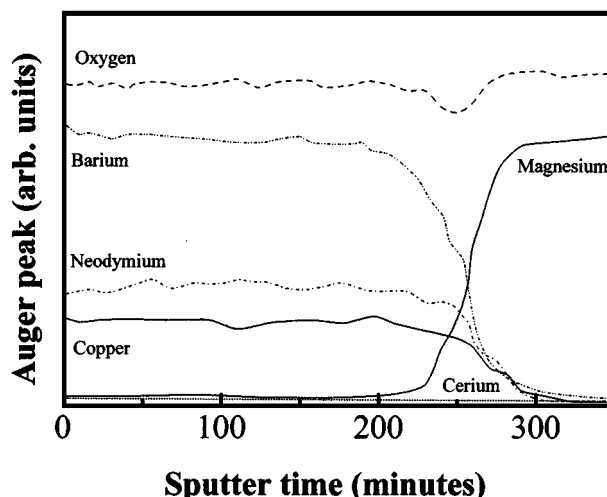


Figure 12 Auger electron spectroscopy depth profile of NdBaCuO film on a MgO substrate (a) with a CeO<sub>2</sub> buffer layer and (b) without a CeO<sub>2</sub> buffer layer.

between NdBaCuO and CeO<sub>2</sub> is negligibly small. Consequently, it was found that the CeO<sub>2</sub> buffer layer is useful for the tunnel barrier needs in superconductor/insulator/superconductor devices.

#### 4. Conclusions

Superconducting thin films of YBaCuO and NdBaCuO were grown by mist microwave-plasma chemical vapor deposition (MPCVD) using a CeO<sub>2</sub> buffer layer on a MgO (001) substrate. In this method, the CeO<sub>2</sub> buffer layer was deposited on the MgO (001) substrate

at 1173 K. YBaCuO and NdBaCuO films were then grown at 1073 K and 1223 K, respectively. The  $T_c$  values of the YBaCuO and NdBaCuO films obtained on a CeO<sub>2</sub> buffer layer were 90.1 K and 94.1 K, respectively. These  $T_c$  values were about 10 K higher than those without a CeO<sub>2</sub> buffer layer. The surface roughness of the YBaCuO and NdBaCuO films obtained were less than 5 nm in each case. The interdiffusion of elements between the substrate and the grown layer was confirmed to be negligibly small by Auger electron spectroscopy. In addition, it was found that the CeO<sub>2</sub> buffer layer played an important role in the improvement of the

crystal quality of the YBaCuO and NdBaCuO films. These results show that MPCVD using a CeO<sub>2</sub> buffer layer is a useful method for growing high-quality superconducting thin films.

## References

1. X. D. WU, R. C. DYE, R. E. MUENCHAUSEN, S. R. FOLTYN, M. MALEY, A. D. ROLLET, A. R. GARCIA and N. S. NOGAR, *Appl. Phys. Lett.* **58** (1991) 2165.
2. J. TANIMURA, K. KURODA, M. KATAOKA, O. WADA, T. YAKAMI, K. KOJIMA and T. OGAWA, *Jpn. J. Appl. Phys.* **32** (1993) L254.
3. W. L. HOLSTEIN, L. A. PARISI, D. W. FACE, X. D. WU, S. R. FOLTYN and R. E. MUENCHAUSEN, *Appl. Phys. Lett.* **61** (1992) 982.
4. K. CHAR, M. S. COLCLOUGH, L. P. LEE and G. ZAHARCHUK, *ibid.* **59** (1991) 2177.
5. A. KOUKITU, Y. HASEGAWA, H. SEKI, H. KOJIMA, I. TANAKA and Y. KAMIOKA, *Jpn. J. Appl. Phys.* **28** (1989) L1212.
6. N. TAKAHASHI, A. KOSAKA, A. KOUKITU and H. SEKI, *ibid.* **33** (1994) L1584.
7. N. TAKAHASHI, A. KOUKITU and H. SEKI, *J. Mater. Sci.* **31** (1996) 2897.
8. N. TAKAHASHI, D. KANEMATSU, A. KOUKITU, H. SEKI and Y. KAMIOKA, *Jpn. J. Appl. Phys.* **32** (1993) L1648.
9. N. TAKAHASHI, A. KOUKITU, H. SEKI and Y. KAMIOKA, *J. Cryst. Growth* **144** (1994) 48.
10. N. TAKAHASHI, A. KOUKITU and H. SEKI, *Jpn. J. Appl. Phys.* **33** (1994) 6518.
11. *Idem.*, *J. Cryst. Growth.* **151** (1995) 300.
12. N. TAKAHASHI, N. TAKEDA, A. KOUKITU and H. SEKI, *Jpn. J. Appl. Phys.* **36** (1997) L1133.

*Received 8 December 1998*

*and accepted 22 July 1999*